2007

Testing for Lorentz Violation: Constraints on Standard-Model-Extension Parameters via Lunar Laser Ranging

James B. R. Battat
jbattat@brynmawr.edu, jbattat@brynmawr.edu

John F. Chandler

Christopher W. Stubbs

Custom Citation
J.B.R. Battat, J.F. Chandler, C.W. Stubbs, *Phys. Rev. Lett.* **99**, 241103 (2007).

Testing for Lorentz Violation: Constraints on Standard-Model-Extension Parameters via Lunar Laser Ranging

James B. R. Battat, John F. Chandler, and Christopher W. Stubbs
Harvard-Smithsonian Center for Astrophysics, Cambridge, Massachusetts 02138, USA
(Received 6 September 2007; published 13 December 2007)

We present constraints on violations of Lorentz invariance based on archival lunar laser-ranging (LLR) data. LLR measures the Earth-Moon separation by timing the round-trip travel of light between the two bodies and is currently accurate to the equivalent of a few centimeters (parts in 10^{11} of the total distance). By analyzing this LLR data under the standard-model extension (SME) framework, we derived six observational constraints on dimensionless SME parameters that describe potential Lorentz violation. We found no evidence for Lorentz violation at the 10^{-6} to 10^{-11} level in these parameters. This work constitutes the first LLR constraints on SME parameters.

DOI: 10.1103/PhysRevLett.99.241103 PACS numbers: 04.80.−y, 06.30.Gv, 11.30.Cp

Lorentz symmetry, the idea that physical laws take the same form in any inertial frame, irrespective of the orientation or velocity of the frame, underpins the standard model and both special and general relativity. Attempts to quantize gravity have resulted in theories that allow for violations of Lorentz symmetry [1]. For example, spontaneous Lorentz-symmetry breaking is possible in certain string theories [2]. At the Planck energy, $\sqrt{\hbar c^5/G} \sim 10^{19}$ GeV, the standard model and general relativity (GR) have comparable influence [3]. Lorentz symmetry may not hold in that regime. Although no existing experiment can probe these energies, a Lorentz-symmetry violation may also manifest itself at much lower energies where existing experiments do have sensitivity [4]. At present, no experiment has detected a violation of Lorentz symmetry.

The standard-model extension (SME) is a generalized effective field theory that adds a set of Lorentz-violating terms to the standard model [4]. The theory of the gravitational sector of the SME was developed in [5,6]. The SME provides a framework to analyze and compare the results of Lorentz-symmetry experiments just as the parametrized post-Newtonian (PPN) framework allows for the comparison of tests of gravity [7]. Recent calculations of the observable consequences of Lorentz-symmetry violations in the pure-gravity sector of the minimal SME [6] showed that existing lunar laser-ranging (LLR) data would be sensitive to a subset of the 20 pure-gravity SME parameters. LLR measures the time of flight of photons between a ranging station on the Earth and retroreflectors on the lunar surface [8]. This experiment has been ongoing since the Apollo astronauts landed on the lunar surface in 1969. Over the past 38 years the measurement precision has improved by more than 2 orders of magnitude and currently LLR data can be used to determine the orbit of the Moon around the Earth to a few millimeters, or a few parts in 10^{12} of the total range [9,10]. In this Letter, we present constraints on six linearly independent combinations of pure-gravity sector SME parameters using archival, centimeter-precision LLR data.

A Lorentz violation would manifest itself as oscillatory perturbations to the lunar orbit [6]. In this section, we describe the convention which we have adopted from [6] for our LLR data analysis. To explore these perturbations, we work a Sun-centered celestial-equatorial frame (see Fig. 1). In this system, the Earth's equator defines the XY plane and the Earth's spin angular momentum vector points along the $+\hat{Z}$ direction. The Earth orbits the Sun in a plane (the ecliptic) which is inclined to the XY plane by an angle η (approximately 23.5°). The Earth's orbit intersects the XY plane at two points, called the ascending and descending nodes. In Fig. 1, the Earth is pictured at the descending node, on the negative X axis (note the arrow that indicates the direction of the Earth's motion along its orbit). At this epoch, commonly called the Vernal Equinox, the Sun, from the point of view of the Earth, ascends through the Earth's equatorial plane. The origin of t, our time coordinate (called T in [6]), coincides with the presence of the Earth at the descending node.

Figure 2 depicts the orbit of the Moon about the Earth. The longitude of the ascending node and the inclination of

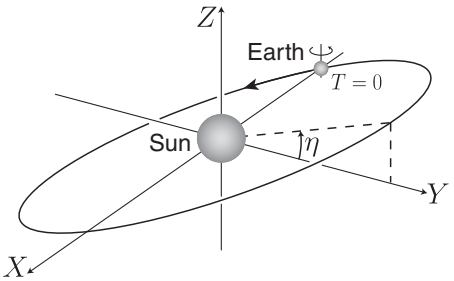

FIG. 1. The Sun-centered celestial-equatorial plane. The equator of the Earth defines the XY plane and the Earth's rotation axis is aligned with the Z axis. The orbital plane of the Earth (the ecliptic) is inclined to the XY plane by the obliquity angle, $\eta \approx 23.5°$. The Earth is shown at a descending node (a Vernal Equniox) which also defines the origin of our time coordinate, t. Reprinted figure with permission from [6]. Copyright 2006 by the American Physical Society.

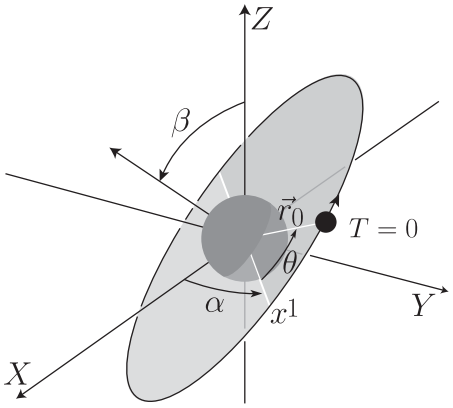

FIG. 2. Lunar orbital parameters: here the Earth is shown translated to the center of the Sun-centered coordinate system. The lunar orbit is described by r_0, the mean distance between the Earth and Moon, e (not labeled) the eccentricity of the lunar orbit, α, the longitude of the ascending node, β, the angle between the normal to the lunar orbital plane and the normal to the Earth's equatorial plane, and θ, the angle, along the Lunar orbit, subtended by the ascending node line and the position of the Moon at $t = 0$. Reprinted figure with permission from [6]. Copyright 2006 by the American Physical Society.

the lunar orbit are labeled α and β, respectively, and r_0 is the mean orbital radius of the Moon. The lunar orbital phase, θ, specifies the position of the Moon along its orbit at the Vernal Equinox epoch ($t = 0$). The eccentricity and longitude of perigee are not specified in this description.

In this coordinate system, Lorentz-violating perturbations to the Earth-Moon separation can be expressed in the SME framework using the following Fourier series:

$$\delta r_{\mathrm{SME}}(t) = \sum_n [A_n \cos(\omega_n t + \phi_n) + B_n \sin(\omega_n t + \phi_n)]. \tag{1}$$

The dominant contributions to $\delta r_{\mathrm{SME}}(t)$ occur at the following four frequencies: ω, 2ω, $2\omega - \omega_0$, and $\Omega_\oplus$. Here (as in [6]) ω is the mean lunar orbital (sidereal) frequency, ω_0 is the anomalistic lunar orbital frequency (perigee to perigee), and $\Omega_\oplus$ is the mean Earth orbital (sidereal) frequency. The corresponding amplitudes (A_n and B_n) and phases (ϕ_n) for these frequencies are listed in Table I. The dominant perturbations to the lunar orbit are controlled by a set of six linearly independent combinations of Lorentz-violating SME parameters, $\bar{s}_{\mathrm{LLR}} = \{(\bar{s}^{11} - \bar{s}^{22}), \bar{s}^{12}, \bar{s}^{02}, \bar{s}^{01}, \bar{s}_{\Omega_\oplus, c}, \bar{s}_{\Omega_\oplus, s}\}$ (see [6] for a description of these parameters).

At present the only published constraints on the gravitational sector SME parameters come from measurements of the perihelion shifts of Mercury and the Earth and from an argument based on the current close alignment of the solar spin axis and the angular momentum vector of the planetary orbits [6]. This Letter provides the first LLR constraints on SME parameters.

TABLE I. The leading-order amplitudes from Eq. (1) and their associated phases (from [6]). M and δm are the sum and difference of the Earth and Moon masses, while $V_\oplus$ and v_0 are the mean Earth and Moon orbital velocities, respectively, normalized to the speed of light. The unitless parameters b_1 and b_2 are functions of η, α, β, r_0, $\Omega_\oplus$, and the Earth's quadrupole moment.

	Amplitudes (A_n, B_n)	Phases (ϕ_n)
$A_{2\omega}$	$-\frac{1}{12}(\bar{s}^{11} - \bar{s}^{22})r_0$	2θ
$B_{2\omega}$	$-\frac{1}{6}\bar{s}^{12}r_0$	2θ
$A_{2\omega-\omega_0}$	$-\omega e r_0(\bar{s}^{11} - \bar{s}^{22})/16(\omega - \omega_0)$	2θ
$B_{2\omega-\omega_0}$	$-\omega e r_0 \bar{s}^{12}/8(\omega - \omega_0)$	2θ
A_ω	$-\omega(\delta m)v_0 r_0 \bar{s}^{02}/M(\omega - \omega_0)$	θ
B_ω	$\omega(\delta m)v_0 r_0 \bar{s}^{01}/M(\omega - \omega_0)$	θ
$A_{\Omega_\oplus}$	$V_\oplus r_0(b_1/b_2)\bar{s}_{\Omega_\oplus c}$	0
$B_{\Omega_\oplus}$	$V_\oplus r_0(b_1/b_2)\bar{s}_{\Omega_\oplus s}$	0

The fundamental LLR observable is the travel time of light (usually a pulsed laser beam) that is propagated from a transmit station on the Earth to one of the retroreflector arrays on the lunar surface and is reflected back to a receive station on the Earth. Typically the receive station is the same as the transmit station. The return signal from the Moon is weak—typically 1 to 5 photons per minute for the data used here—and single-photon counters are required to detect and time-tag lunar reflection events.

LLR data have historically been presented as "normal points" which combine a series of single-photon lunar reflection events to achieve a higher signal-to-noise ratio measurement of the lunar range at some characteristic epoch for that data series. In this analysis, we used 14 401 normal points spanning September 1969 through December 2003, taken from the public LLR data archive [11]. The bulk of these normal points were generated by the McDonald Laser-Ranging Station in Texas, USA [12] and the Observatoire de la Côte d'Azur (OCA) station in Grasse, France [13]. A single normal point is typically generated from an observation spanning 5 to 20 minutes during which anywhere from a few to a hundred photons are collected. The lunar ranges reported in these normal points incorporate station-specific hardware corrections.

In order to analyze LLR data, one relies on detailed models of the solar system ephemeris. To our knowledge, there are only a few such models in existence capable of this analysis [8,14–16]. None of these codes explicitly include the SME framework in their equations of motion for solar system bodies. But it is possible to use them to constrain the $\bar{s}_{\mathrm{LLR}}$ parameters.

We used the Planetary Ephemeris Program (PEP) [15] to extract SME parameter constraints from LLR observations. PEP uses its ephemeris model, along with an initial set of model parameters, to compute a range prediction and the partial derivatives of range with respect to each model parameter at the epoch of each normal point. It then

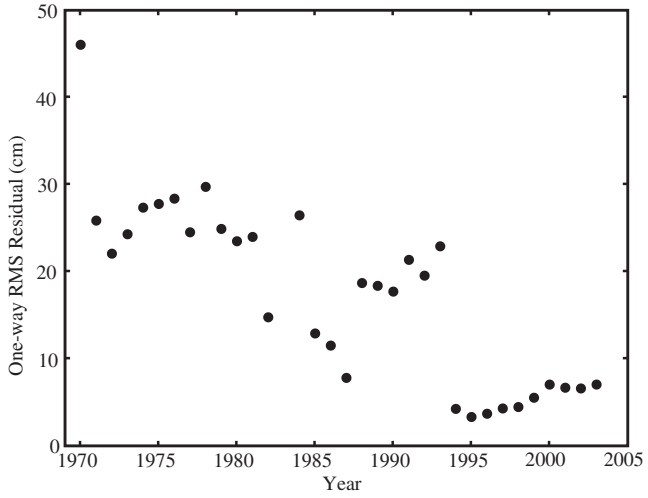

FIG. 3. The annual RMS residual between the LLR data and our best-fit model for the lunar range. The residual RMS in 1969 is over 300 cm. We omitted this point from the plot for clarity, but the two data points from that year were included in the analysis. Over this time span, the potential Lorentz-violating signals would all have undergone at least 34 cycles. As the number and capability of LLR ranging stations change with time so too does the LLR data rate and quality. For example, the sharp improvement in the model-data agreement around 1995 is due to the upgrade of the OCA station.

performs a weighted, linear least-squares analysis to calculate adjustments to the model parameters in order to minimize the difference between the observations and the model.

If one is concerned about nonlinearities, one can solve for model parameters and then reintegrate the equations of motion, iterating until the parameter estimates converge. Over the past several decades the traditional (i.e., non-SME) analyses have done just that, resulting in agreement between model and data at the few centimeter level. Current model parameter values are therefore highly refined, and the weighted least-squares analysis sits firmly in the linear regime. As a result, it is not necessary to iterate when estimating new model parameters. Because the lunar range model is linear in the $\bar{s}_{\mathrm{LLR}}$ parameters [see Eq. (1) and Table I], the inclusion of these parameters in the analysis preserves linearity, as confirmed by the small adjustments to non-SME parameters seen in our solutions. Performing an iterative solution for SME parameters requires the inclusion of the SME terms in the equations of motion, which has not yet been done.

We computed the partial derivatives of lunar range with respect to each $\bar{s}_{\mathrm{LLR}}$ parameter (see Table II) and provided this information to PEP prior to solving for the best-fit parameter adjustments. This approach is equivalent to explicitly including the $\bar{s}_{\mathrm{LLR}}$ parameters in the equations of motion and setting their *a priori* values to zero [in which case $\delta r_{\mathrm{SME}}(t) = 0$ so there is no SME contribution to the lunar orbit]. We therefore treated any Lorentz violation as a small perturbation to a known orbit. The terms in the covariance matrix quantify "cross-talk" between SME parameters and other fitted quantities.

TABLE II. The partial derivatives of the SME perturbation to the lunar range with respect to each $\bar{s}_{\mathrm{LLR}}$ parameter.

SME parameter partial derivatives
$\frac{\partial \delta r}{\partial(\bar{s}^{11}-\bar{s}^{22})} = -\frac{r_0}{12}\cos(2\omega t + 2\theta) - \frac{\omega e r_0}{16(\omega-\omega_0)}\cos[(2\omega-\omega_0)t + 2\theta]$
$\partial\delta r/\partial\bar{s}^{12} = -\frac{r_0}{6}\sin(2\omega t + 2\theta) - \frac{\omega e r_0}{8(\omega-\omega_0)}\sin[(2\omega-\omega_0)t + 2\theta]$
$\partial\delta r/\partial\bar{s}^{02} = -\frac{\omega(\delta m)v_0 r_0}{M(\omega-\omega_0)}\cos(\omega t + \theta)$
$\partial\delta r/\partial\bar{s}^{01} = \frac{\omega(\delta m)v_0 r_0}{M(\omega-\omega_0)}\sin(\omega t + \theta)$
$\partial\delta r/\partial\bar{s}_{\Omega_\oplus c} = V_\oplus r_0(\frac{b_1}{b_2})\cos(\Omega_\oplus t)$
$\partial\delta r/\partial\bar{s}_{\Omega_\oplus s} = V_\oplus r_0(\frac{b_1}{b_2})\sin(\Omega_\oplus t)$

The solar system is complex. When modeling the expected light travel time between an LLR station on the Earth and a reflector on the lunar surface, one must account not only for the gravitational perturbations from the eight planets and Pluto, but also those of asteroids, asphericities in the Sun, Earth, and Moon, as well as various relativistic and nongravitational effects (for a more complete description of relevant physical effects, see [8]). As a result there are many hundreds of parameters that have influence on the Earth-Moon range time. Not surprisingly, there are parameter-estimate degeneracies and LLR data alone cannot determine all of these parameters. Therefore, LLR-only analyses suffer from systematic uncertainties in model parameter estimates, and the standard deviations (formal errors) reported by the least-squares solution will underestimate the true model parameter-estimate uncertainties. These systematic contributions to the uncertainties can dominate the formal errors. If auxiliary solar system data is included in the analysis (e.g., planetary radar ranging), then the number of model parameters grows and new parameter-estimate degeneracies arise. Having chosen to

TABLE III. The predicted sensitivity to each $\bar{s}_{\mathrm{LLR}}$ parameter (from [6]) and the values derived in this work including the realistic (scaled) uncertainties ($F\sigma$) with $F = 20$. In this analysis, the PPN parameters were fixed at their GR values. The SME parameters are all within 1.5 standard deviations of zero. We see no evidence for Lorentz violation under the SME framework.

Parameter	Predicted sensitivity	This work
$\bar{s}^{11}-\bar{s}^{22}$	10^{-10}	$(1.3 \pm 0.9) \times 10^{-10}$
$\bar{s}^{12}$	10^{-11}	$(6.9 \pm 4.5) \times 10^{-11}$
$\bar{s}^{02}$	10^{-7}	$(-5.2 \pm 4.8) \times 10^{-7}$
$\bar{s}^{01}$	10^{-7}	$(-0.8 \pm 1.1) \times 10^{-6}$
$\bar{s}_{\Omega_\oplus c}$	10^{-7}	$(0.2 \pm 3.9) \times 10^{-7}$
$\bar{s}_{\Omega_\oplus s}$	10^{-7}	$(-1.3 \pm 4.1) \times 10^{-7}$

perform our analysis using LLR data alone, we accounted for the underestimation of parameter uncertainties by inflating the formal parameter uncertainties from our least-squares solution by a uniform factor which we label F. This is numerically equivalent to a uniform scaling of the uncertainty associated with each normal point by F.

In order to determine the F factor, we performed an analysis of the LLR data in which we froze all $\bar{s}_{\mathrm{LLR}}$ parameters at zero, but allowed the PPN parameters, β and γ, to vary. We know from other experiments [9,17–19] that β and γ are consistent with their GR value of unity to within a part in 10^3 or better. We found that we must scale our uncertainties on β and γ by $F = 20$ to be in accord with these earlier results.

We then estimated the values of the set of $\bar{s}_{\mathrm{LLR}}$ parameters while holding the PPN parameters at their GR values ($\beta = \gamma = 1$). The resulting parameter values and their realistic errors (the formal errors scaled by the $F = 20$ factor) are reported in Table III. All SME parameters are within one and a half standard deviations of zero and are within an order of magnitude of the sensitivity expected from 1 cm precision LLR data as estimated in [6]. There is no evidence for Lorentz violation in the lunar orbit. The model-data agreement, binned annually, is shown in Fig. 3.

To ensure that our analysis is sensitive to the signature of a Lorentz violation in the lunar range, we generated a perturbed LLR data set with a hand-inserted Lorentz-violation signal corresponding to a value of $\bar{s}^{11} - \bar{s}^{22} = 9 \times 10^{-10}$ (a factor of 10 larger than the uncertainty for this parameter). Our analysis recovers this signal. We found $\bar{s}^{11} - \bar{s}^{22} = (10 \pm 0.9) \times 10^{-10}$ (here, the reported uncertainty has been scaled by F as before) with the other $\bar{s}_{\mathrm{LLR}}$ parameters unchanged.

In conclusion, we have analyzed over 34 years of archival LLR data using PEP to derive constraints (see Table III) on six linearly independent Lorentz-violation parameters in the pure-gravity sector of the SME. These are the first LLR-based SME constraints. Using the same LLR data set, these constraints could be improved by performing a simultaneous fit with auxiliary solar system data to help break parameter-estimate degeneracies and thereby reduce the systematic error budget. We estimate that the SME parameter constraints could be improved by a factor of 5–10 with a joint fit. In addition, we are involved in the Apache Point Observatory Lunar Laser-Ranging Operation Project (APOLLO), a next-generation LLR station that is currently collecting millimeter-precision lunar range data [10]. We plan to improve the SME parameter constraints by incorporating APOLLO data into our analysis.

This project developed out of conversations with several colleagues including E. Adelberger, Q. Bailey, J. Davis, A. Kostelecký, J. Moran, T. Murphy, I. Shapiro, and M. Zaldarriaga. We would also like to thank the LLR observers and the ILRS for the data collection and normal point distribution. J. B. R. B. acknowledges financial support from the ASEE NDSEGF, the NSF GRFP, and Harvard University. Generous financial support was provided by the National Science Foundation (Grant No. PHY-0602507).

[1] G. Amelino-Camelia *et al.*, AIP Conf. Proc. **758**, 30 (2005).
[2] V. A. Kostelecký and S. Samuel, Phys. Rev. D **39**, 683 (1989).
[3] J. H. Schwarz and N. Seiberg, Rev. Mod. Phys. **71**, S112 (1999).
[4] D. Colladay and V. A. Kostelecký, Phys. Rev. D **58**, 116002 (1998).
[5] V. A. Kostelecký, Phys. Rev. D **69**, 105009 (2004).
[6] Q. G. Bailey and V. A. Kostelecký, Phys. Rev. D **74**, 045001 (2006).
[7] C. Will and K. Nordtvedt, Astrophys. J. **177**, 757 (1972).
[8] J. G. Williams, S. G. Turyshev, and D. H. Boggs, arXiv:gr-qc/0507083.
[9] J. G. Williams, S. G. Turyshev, and D. H. Boggs, Phys. Rev. Lett. **93**, 261101 (2004).
[10] T. W. Murphy *et al.* (to be published).
[11] M. R. Pearlman *et al.*, Adv. Space Res. **30**, 135 (2002).
[12] P. J. Shelus *et al.*, *IAU Symposium*, edited by S. Ferraz-Mello *et al.* (Kluwer Academic Publishers, Dordrecht, 1996), Vol. 172, p. 409.
[13] E. Samain *et al.*, Astron. Astrophys. Suppl. Ser. **130**, 235 (1998).
[14] J. Müller *et al.*, in *Proceedings of the 7th Marcel Grossman Meeting on General Relativity*, edited by R. T. Jantzen, G. Mac Keiser, and R. Ruffini (World Scientific, Singapore, 1996), p. 1517.
[15] The Planetary Ephemeris Program is a solar system ephemeris and data analysis program that was developed at the Massachusetts Institute of Technology and its Lincoln Laboratory, beginning in the early 1960s. The source code is currently maintained by John Chandler at the Center for Astrophysics in Cambridge, MA and is publicly available.
[16] E. V. Pitjeva, Solar System Research **39**, 176 (2005).
[17] B. Bertotti *et al.*, Nature (London) **425**, 374 (2003).
[18] S. S. Shapiro *et al.*, Phys. Rev. Lett. **92**, 121101 (2004).
[19] J. F. Chandler *et al.*, in *Proceedings of the 7th Marcel Grossman Meeting on General Relativity*, edited by R. T. Jantzen, G. Mac Keiser, and R. Ruffini (World Scientific, Singapore, 1996), p. 1501.